

Identification of Volterra Models of Tube Audio Devices Using Multiple-Variance Method

SIMONE ORCIONI¹, **ALESSANDRO TEREZI¹**, *AES Student Member*,
(s.orcioni@univpm.it) (a.terenzi@staff.univpm.it)

STEFANIA CECCHI¹, *AES Associate Member*, **FRANCESCO PIAZZA¹**, *AES Associate Member*, **AND**
(s.cecchi@univpm.it) (f.piazza@univpm.it)

ALBERTO CARINI²
(alberto.carini@uniurb.it)

¹*Department of Information Engineering (DII), Università Politecnica delle Marche, Ancona, Italy*

²*Department of Pure and Applied Sciences, University of Urbino, Urbino, Italy*

The multiple-variance method is a cross-correlation method that exploits input signals with different powers for the identification of a nonlinear system by means of the Volterra series. It overcomes the problem of the locality of the solution of traditional nonlinear identification methods, based on mean square error minimization or cross-correlation, that well approximate the system only for inputs that have approximately the same power of the identification signal. The multiple-variance method permits to improve the performance of models of systems that have inputs with high dynamic, like audio amplifiers. This method is used, for the first time, to identify three different tube amplifiers. The method is applied to a novel reduced Volterra model that allows to overcome the problem of the very large number of coefficients required by the Volterra series by choosing only a proper subset of elements from each kernel. Eventually, the multiple-variance methodology is applied to different real audio tube devices demonstrating the effectiveness of the proposed approach in terms of system identification and computational complexity.

0 INTRODUCTION

The paper addresses the problem of the locality of the solution in the identification of nonlinear systems with the Volterra series. The problem affects most of traditional identification methods based on mean square minimization or cross-correlation, which well approximate the system only for inputs that have approximately the same power of the identification signal. The Volterra series is a polynomial functional series for nonlinear system representation and identification, extending to functionals the Taylor series expansion [1]. It owes its spread of use in engineering to the work of Norbert Wiener on Brownian motion linear transformation, on higher degree functionals of Brownian motion, and their orthogonalization [2]. Along with the work of his colleagues [3], Wiener continued to develop his theories by combining Volterra series and his previous works, and finally defining the so called Wiener series. In real application the Wiener's method was difficult to implement due to the use of Brownian motion, so a further step in its usability came from the work of Lee and Schetzen [4], who developed a method that uses white Gaussian noise

as input and cross-correlation for parameter estimation of Wiener series coefficients, the so called cross-correlation method. Exploiting the relationship between Wiener and Volterra coefficients, it is then possible to obtain an equivalent Volterra series from the Wiener series.

While in the early works the Volterra series was considered an analytical power series (infinite sum of elements) defined in the continuous-time domain, current interest is addressed to the discrete-time series, truncated in both memory and order of nonlinearity, generally called double truncated Volterra series. Considering the identification of systems with finite memory, using the Stone-Weierstrass theorem [5] it can be demonstrated that the approximation error can be made arbitrary small increasing the order and memory of the truncated series, and in this sense the Volterra series is a universal approximator.

While in the analytical continuous-time power series the identification using the cross-correlation method is independent of input variance, in truncated discrete-time series this is no longer true. The approximation error now depends on the input variance used in the identification [6, 7], originating the problem of the locality of the

solution. A Volterra series can be considered optimal only for inputs with variances in a neighborhood of that used for identification, either performed with a cross-correlation or a least mean square based method [8]. An improved cross-correlation method for nonlinear system identification based on multiple-variances has been proposed for Wiener-Volterra series and Gaussian input in [8]: low input variances are used to identify lower order Wiener kernels, while the input variance is gradually increased for higher order kernels.

In [9] the Wiener series was expressed as a linear combination of Wiener nonlinear (WN) basis functions, which are orthogonal for white Gaussian inputs. Deterministic periodic signals, called perfect periodic sequences (PPSs), that guarantee the orthogonality of the basis functions on a finite period, can also be developed. Using a PPS input signal, the identification of an unknown nonlinear filter can be improved either by using Wiener kernels or Wiener basis functions as approximators [9, 10].

In a multiple-variance method, the different input variances allow to reach a lower error than the traditional identification for a wide range of input dynamics. So this method is specifically targeted to the identification of systems having high dynamic inputs, like audio amplifiers.

In this paper a detailed analysis of a multiple-variance method applied to tube devices will be performed. In this context, a well known limitation of Volterra series is the very large number coefficients involved [11], which increases exponentially with the filter order and geometrically with the memory length. We will show that this serious drawback can be overtaken by choosing only a subset of elements from each full memory kernel. The subset is obtained by delaying and reducing the memory of the identified nonlinear kernels, i.e., considering only the most relevant terms of each kernel. The estimation of the reduced kernel can still be done with the cross-correlation estimation method, as proposed in [10], since with the cross-correlation method each kernel element is estimated independently of other elements. In this way, it will be shown that it is possible to obtain a good approximation error also with a reduced number of kernel elements on an extended range of input signal variances. Experimental results involving real nonlinear audio devices, i.e., tube amplifiers and pre-amplifiers, will illustrate the advantages offered by the proposed approach.

The paper is organized as follows. Sec. 1 will discuss related works based on nonlinear system identification for real audio devices. The multiple-variance method will be described in Sec. 2, while experimental results will be reported in Sec. 3 considering several tube devices, i.e., audio amplifiers and pre-amplifiers. Finally, concluding remarks will be given in Sec. 4.

1 RELATED WORKS

In the past years, several different approaches have been investigated in order to develop a technique suitable for an efficient modeling of tube audio devices [12]. These approaches can be divided into three main categories: the white box approach where the system structure is known

(e.g., the schematic of an amplifier is available), the black box approach where the system is totally unknown and only the inputs/outputs are available, the gray box approach where the structure is not completely known but some features are available and could be used to improve the model. Typically, white box approaches are used to approximate the amplifier circuit gain stage exploiting differential equations [13] or the wave digital filters [14, 15], obtaining a complete mathematical model of real devices. On the other hand, the gray or black box approaches are based on well known models, such as the Hammerstein model [11, 16–17], Wiener model [11, 17], Wiener Hammerstein model [11, 18], and the Volterra series, that are identified exploiting particular input signals (e.g., exponential sine sweep). Starting from the input/output characteristic and a block diagram of the analog circuit, an iterative parameter optimization has been also considered in [19, 20], to model a dynamic range compression system. To the gray box approaches belongs also the Significance Aware Filtering concept [21–24] introduced in the field of nonlinear acoustic echo control, where the long memory nonlinear acoustic system is decomposed into synergetic subsystems, separating the long memory linear system representing the acoustic echo path from a nonlinear part composed by a very low number of parameters. An example of a black box approach can be found in [25] where a Volterra series with kernels expressed as products of one-dimensional functions has been used for modeling a surround amplifier. Considering the nonlinear identification of other audio devices, several techniques have been applied for the identification of guitar pedal distortion effects [26–29, 12] or nonlinear guitar speaker cabinet [30]. Regarding the pedal distortion emulation, a methodology based on Volterra series has been introduced in [26], exploiting its expansion to approximate the circuit nonlinear part, e.g., the asymmetric distortion produced by a triode valve or by a saturated operational amplifier. In a similar way, a parametric Wiener Hammerstein model exploiting an iterative algorithm has been used in [27] for guitar stompbox identification. In case of simple circuits such as the overdrive or distortion guitar pedal, approaches based on physical modeling have also been studied. In [28] the circuit is approximated exploiting a nonlinear state-space model, while in [29] the circuit elements are approximated by means of numerical solutions of ordinary differential equations. Taking into consideration the speaker cabinet of electric guitars, the Volterra kernels have been used for the cabinet approximations in [30] exploiting a logarithmic sine sweep technique, which provides a way to separate the different orders of Volterra Kernels from the linear part.

With relation to nonlinear digital effects, in [31] it is shown how the formalism of the Volterra series can be used to represent the nonlinear Moog ladder filter. In this case using a truncated version of Volterra series allows to develop a model for an extended range of input signals.

Then, nonlinear system identification can also be applied to loudspeaker development: the nonlinear model can be used to design an equalization filter capable of reducing the device nonlinearity. In [32], a Volterra series has been

applied to estimate the nonlinearity of a horn loudspeaker, while in [33] it is shown how to reduce the identified non-linearity developing an equalization filter. A different technique is the nonlinear autoregressive moving average with exogenous input (NARMAX) model, originally proposed in [34], that has been used in [35, 36] to model loudspeaker nonlinearities.

Taking into consideration the overall scenario of digital music, in [37] a method for band-limited discrete-time identification and modeling of analog nonlinear audio effects, like tube amps, exciters, etc., has been presented using off-time digital cross correlation measurements. Finally considering more classical musical instruments, the Volterra series representation has also been used to obtain a model of nonlinear behavior of instruments such as an ocarina in [38] or a more conventional flute in [39].

2 MULTIPLE-VARIANCE METHOD

In [8] the author shows a strong dependence between the power of the white noise (σ_x^2), used to identify a Volterra series, and the approximation capability of model itself, independently from the algorithm used in the identification. The Volterra series, tested with different power inputs, shows an increasing error as the input power increases or decreases with respect to that used in the identification. This happens because several errors affecting the identification of the Volterra series depend on the input power. The cause of these errors can be related to the input non-idealities and to the approximation errors due to the double truncation of the series, with respect to memory and order of nonlinearity [7]. In traditional algorithms, using high σ_x inputs has the advantage of stimulating higher order nonlinearities, in order to achieve more accurate higher order kernel identification. As a drawback, the use of high σ_x values causes high identification errors in lower order kernels, since the higher order Wiener kernels, multiplied by the variances of lower order kernels, are summed to the lower order Volterra kernels [8].

The rationale should be to use a low σ_x value for the lower order kernels and to gradually increase it for higher order ones. This is the core of the multiple-variance method, where inputs with different variances are used for Wiener kernel identification, allowing to reach a lower error with respect the traditional identification for inputs with wide dynamics.

We can start by introducing the double truncated Volterra series that models a discrete time, nonlinear, finite memory system

$$y(n) = h_0 + \sum_{i=1}^P (H_i x)(n), \quad (1)$$

$$(H_i x)(n) = \sum_{\tau_1=0}^M \sum_{\tau_2=\tau_1}^M \cdots \sum_{\tau_i=\tau_{i-1}}^M h_i(\tau_1, \dots, \tau_i) \times \prod_{j=1}^i x(n - \tau_j),$$

where $y(n)$ is the output of the system, $x(n)$ its input, and $h_i(\tau_1, \dots, \tau_i)$ is the Volterra kernel of order i . The output $y(n)$ is a linear combination of product of delayed input samples, where the delays τ_j are also the indexes of the kernel matrices $h_i(\tau_1, \dots, \tau_i)$.

In order to allow system identification by means of a cross-correlation method the Volterra series must be rearranged in terms of orthogonal operators:

$$y(n) = \sum_i (H_i x)(n) \equiv \sum_i (G_i x)(n). \quad (2)$$

These operators, commonly known as Wiener G-functionals, are orthogonal to each other and also to Volterra operators of lower orders if the input $x(n)$ is a stationary white noise with zero mean and variance σ_x^2 . The Wiener G-functionals, unlike the Volterra ones, are non-homogeneous functionals, being a linear combination of polynomial terms of different orders. The Wiener kernels can be identified by means of the multiple variance method with the formulas presented in [8] that are explicitly reported in the following up to the fourth order,

$$k_0^{(0)} = E[y^{(0)}(n)], \quad (3)$$

$$k_1^{(1)}(\tau_1) = \frac{1}{A_1} E[y^{(1)}(n)x^{(1)}(n - \tau_1)], \quad (4)$$

$$k_2^{(2)}(\tau_1, \tau_2) = \frac{1}{2!A_2^2} \left\{ E \left[y^{(2)}(n) \prod_{i=1}^2 x^{(2)}(n - \tau_i) \right] - A_2 k_0^{(2)} \delta_{\tau_1 \tau_2} \right\}, \quad (5)$$

$$k_3^{(3)}(\tau_1, \tau_2, \tau_3) = \frac{1}{3!A_3^3} \left\{ E \left[y^{(3)}(n) \prod_{i=1}^3 x^{(3)}(n - \tau_i) \right] - A_3^2 \left[k_1^{(3)}(\tau_1) \delta_{\tau_2 \tau_3} + k_1^{(3)}(\tau_2) \delta_{\tau_1 \tau_3} + k_1^{(3)}(\tau_3) \delta_{\tau_1 \tau_2} \right] \right\}, \quad (6)$$

$$k_4^{(4)}(\tau_1, \tau_2, \tau_3, \tau_4) = \frac{1}{4!A_4^4} \left\{ E \left[y^{(4)}(n) \prod_{i=1}^4 x^{(4)}(n - \tau_i) \right] - A_4^2 \left[k_2^{(4)}(\tau_1, \tau_2) \delta_{\tau_3 \tau_4} + k_2^{(4)}(\tau_1, \tau_3) \delta_{\tau_2 \tau_4} + k_2^{(4)}(\tau_1, \tau_4) \delta_{\tau_2 \tau_3} + k_2^{(4)}(\tau_2, \tau_3) \delta_{\tau_1 \tau_4} + k_2^{(4)}(\tau_2, \tau_4) \delta_{\tau_1 \tau_3} + k_2^{(4)}(\tau_3, \tau_4) \delta_{\tau_1 \tau_2} \right] \right\}, \quad (7)$$

where $k_p^{(j)}$ and $y^{(j)}(n)$ are respectively the Wiener kernel of order p and the system output obtained with the input $x^{(j)}(n)$ of variance $A_j = \sigma_{x^{(j)}}^2$. In the cross-correlation method the expectations in Eqs. (3)–(7) are estimated using time averages over the entire duration of the input and output signal.

Wiener kernels can now be rearranged to obtain directly the expression of the Volterra kernels and so the Volterra

series. Appropriate normalization is needed in Wiener to Volterra conversion formulas, unlike in the usual ones, for taking into account the use of multiple variances. The new formulas for the changeover from Wiener to Volterra are reported in the following equations,

$$h_4 = k_4^{(4)}, \quad (8)$$

$$h_3 = k_3^{(3)}, \quad (9)$$

$$h_2 = k_2^{(2)} - 6A_2 \sum_{\tau_3=0}^{M-1} k_4^{(4)}(\tau_1, \tau_2, \tau_3, \tau_3), \quad (10)$$

$$h_1 = k_1^{(1)} - 3A_1 \sum_{\tau_2=0}^{M-1} k_3^{(3)}(\tau_1, \tau_2, \tau_2), \quad (11)$$

$$h_0 = k_0^{(0)} - A_0 \sum_{\tau_1=0}^{M-1} k_2^{(2)}(\tau_1, \tau_1) + 3A_0^2 \sum_{\tau_1=0}^{M-1} \sum_{\tau_2=0}^{M-1} k_4^{(4)}(\tau_1, \tau_1, \tau_2, \tau_2), \quad (12)$$

where all kernels have memory equal to M , and the system has a maximum order $P = 3$.

The following formula

$$N = \binom{M+P}{P}, \quad (13)$$

gives the total number of coefficients of a Wiener or Volterra truncated series, when all kernels have the same memory. Eq. (13) provides the well known exponential relationship used by all papers in support of the curse of dimensionality of Volterra series.

The curse can be broken by simply avoiding the kernels to have the same memory and above all avoiding to have the same memory of the first order one. A procedure for estimating the kernels of nonlinear audio devices with a symmetric distribution of the coefficients around the main peak, as in audio amplifiers, is discussed in the following. The procedure could be easily modified to address also asymmetric distributions and it consists of the following parts:

- The identification of the first order kernel is carried out using Eq. (3) with a large memory, since it is not computationally expensive. Then M_1 is chosen by discarding all negligible kernel values, i.e., those under the noise floor.
- From the first order impulse response the delay of the main peak, P_1 , is estimated.
- Higher order kernels are identified with Eqs. (3)–(7), starting by kernels with an memory M_p equal to a fraction of M_1 and centered at P_p equal to P_1 .
- M_p can be now increased (or, if needed, reduced) by a steepest descent procedure, until the performance of the Volterra model is not satisfactory.

Table 1. Experiments Summary

| Device Type | Number of input variances | | |
|-------------|---------------------------|-------|-------|
| | Identification Noise | Test | |
| | | Noise | Music |
| Synthesis | 4 | 13 | 13 |
| SI Audio | 5 | 13 | 13 |
| Presonus | 4 | 13 | 13 |

With this procedure the delay of the first kernel value different from zero is

$$D_p = P_p - M_p/2. \quad (14)$$

The delay D_p and the memory M_p changes for each kernel. In the experimental part we will show that with the proposed technique we can obtain a complexity reduction of one order of magnitude for a third order system and of two orders of magnitude for a fourth order system.

3 EXPERIMENTAL RESULTS

In this section two experiments were conducted on each of the three different tube audio devices:

1. Identification and test of one complete multiple-variance and four complete single-variance Volterra models in order to prove that the multiple-variance model performs better, for a wide range of input powers, than the single-variance models;
2. Identification and test of reduced-kernel models to prove that the reduced models perform comparably to the complete ones and that also in this case the multiple-variance performs better than the single-variance ones.

The description of the measurement set-up and of the obtained results will be reported in the following subsections.

3.1 Measurement Set-Ups

The proposed methodology has been tested with three different vacuum-tube amplifiers as reported in Table 1. Two set-ups have been considered: the first one with HI-FI vacuum-tube amplifiers, the latter with a microphone tube pre-amplifier.

In the first setup, the SI Audio OTL509/25 and the Synthesis Roma 27AC amplifiers have been used. Both the amplifiers have been connected to a pair of Auna 501 passive 2-way speakers with an RMS rated power of 100 W, an impedance of 8 Ω , and a frequency range of 92 Hz – 20 kHz. The volume has been set at the highest value and after half an hour of warm up, the input signal has been applied with a 6 dB of attenuation of the D/A converter, and the output signal has been measured across the speaker terminals. Even though these two amplifiers are based on tube technology, they show a different circuit: the SI Audio amplifier is an all triode OTL Amplifier (output

transformerless), while the Synthesis amplifier shows a more conventional architecture, with an output transformer.

In the second setup, a microphone tube preamplifier, i.e., Presonus TubePre, has been used connecting it in loop with the measurement setup with an unbalanced cable. The TubePre uses a triode 12AX7 valve, and it allows two main controls: a drive potentiometer that acts on the valve saturation and a gain control that acts on the overall gain of the preamplifier adding more volume and distortion. The drive has been set at 4 dB (within a range from 0 to 20 dB), the gain at 12 dB (within a range from 3 to 48 dB) and the A/D converter attenuation of 20 dB; this setting has low values of drive and gain in order to avoid a too heavy distortion.

For all measurement setup, a National Instruments Compact Rio chassis (cRIO-9024) equipped with a 2-channel voltage analog output NI-9260 and with a 3-channel voltage analog input NI-9232, connected to a desktop PC have been considered. Both generation and acquisition boards have been configured to use the same sample clock with a sample rate of 44100 Hz. The National Instruments software LabView was used to generate the test signals and to acquire the measurements.

Two types of sound tracks have been considered for the measurement. The first, used for the identification procedure, is composed by the concatenation of white noise signals with different power values, interleaved with a 1 s of silence, as shown in Fig. 1(a). The second, used for testing the identified model, is a combination of music and white noise, as shown in Fig. 1(b).

In order to exploit all the resolution of the D/A converter, used to drive the amplifier, the maximum variance in the identification signal was set equal to $1/12$, $\sigma_5^2 = A_5 = 1/12$. With this value only a negligible percentage (0.05%) of noise values saturates the D/A converter, exceeding 1. In the following, the nonlinear devices are modeled with third order or fourth order Volterra systems. Thus, five different input variances were considered to allow the identification of each kernel of a fourth order system at a different input variance. A subset of these input variances will be used for the identification of third order systems.

The set of variances of the five white noises $\{\sigma_1^2, \sigma_2^2, \sigma_3^2, \sigma_4^2, \sigma_5^2\}$ was chosen equal to $\{A_5/64, A_5/16, A_5/8, A_5/2, A_5\}$.

Accordingly, the corresponding numeric values of standard deviations $\{\sigma_1, \sigma_2, \sigma_3, \sigma_4, \sigma_5\}$ are

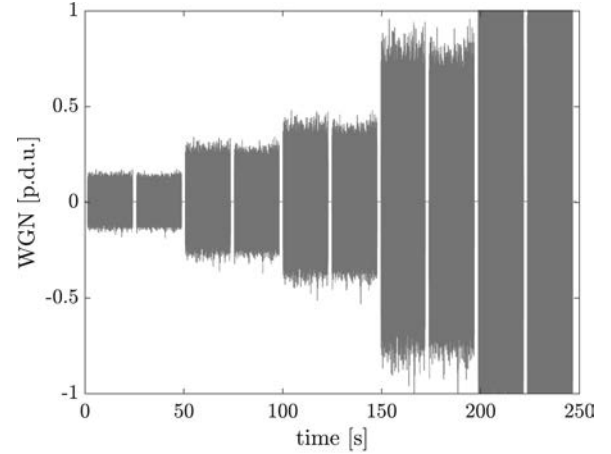
$$\{0.036, 0.0722, 0.102, 0.204, 0.288\}. \quad (16)$$

To test the model performance a normalized mean square error (NMSE) defined over the output spectrogram has been used. To define it formally, let us write

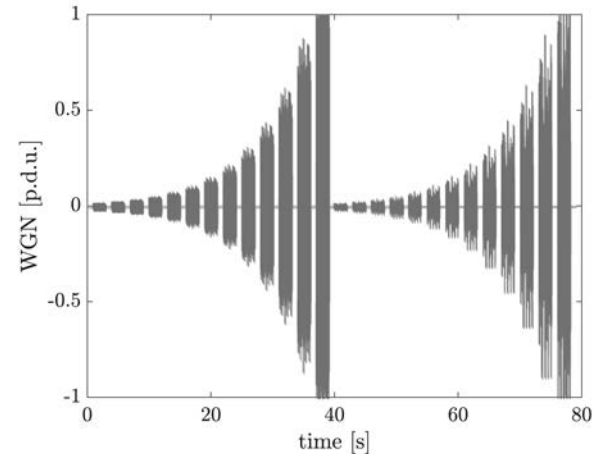
$$Y_A(\tau, \omega) = \text{STFT}[y_A(n)] \quad (17)$$

$$Y_M(\tau, \omega) = \text{STFT}[y_M(n)] \quad (18)$$

where $y_A(n)$ and $y_M(n)$ are the output of the amplifier and of the model, respectively, and the STFT is the Short Time Fourier Transform, calculated using a Hamming window such that the signal is divided into eight segments with



(a)



(b)

Fig. 1. Input signals used (a) for the identification (b) for testing, expressed in procedure defined units (p.d.u.) [40].

50% overlapping samples. The mean square error between two matrices can be defined as

$$\begin{aligned} \text{MSE}[Y_A, Y_M] \\ = \frac{1}{RC} \sum_i \sum_j [Y_A(i, j) - Y_M(i, j)]^2 \end{aligned} \quad (19)$$

where RC is the product between the number of rows and columns of one matrix. Now we are able to define the NMSE as

$$\text{NMSE} = \text{MSE}(|Y_A|, |Y_M|) / \text{MSE}(|Y_A|, 0), \quad (20)$$

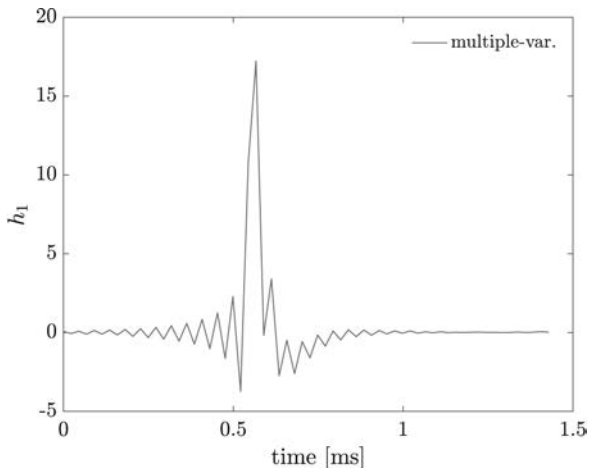
where $|\cdot|$ denotes the magnitude applied to each element of the matrix.

3.2 Synthesis Roma 27AC Identification Results

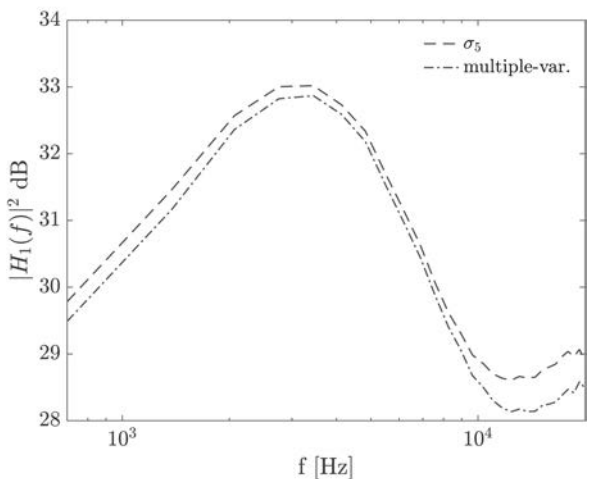
In the first experiment the Roma 27AC vacuum-tube amplifier has been identified. Four Volterra models were identified with the cross-correlation algorithm defined in [7], each model using an input with a different variance belonging to the set in Eq. (15). Then, a single Volterra model was identified with the multiple-variance

Table 2. Variances used in the multiple-variance estimation method.

| kernel | input variance |
|--------|----------------|
| k_0 | σ_1^2 |
| k_1 | σ_2^2 |
| k_2 | σ_4^2 |
| k_3 | σ_5^2 |



(a)



(b)

Fig. 2. Roma 27AC: first order Volterra kernel, (a) in time domain ($h_1(\tau)$) (b) in frequency domain ($|H_1(f)|^2$).

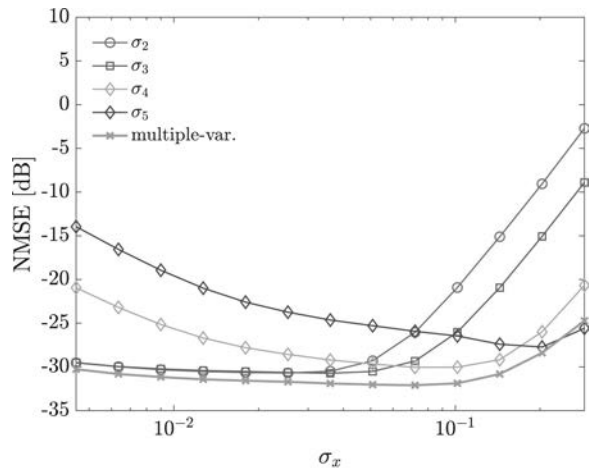
method [8], estimating each Wiener kernel at a different variance as reported in Table 2.

The memory spans of the kernels of all these Volterra models were

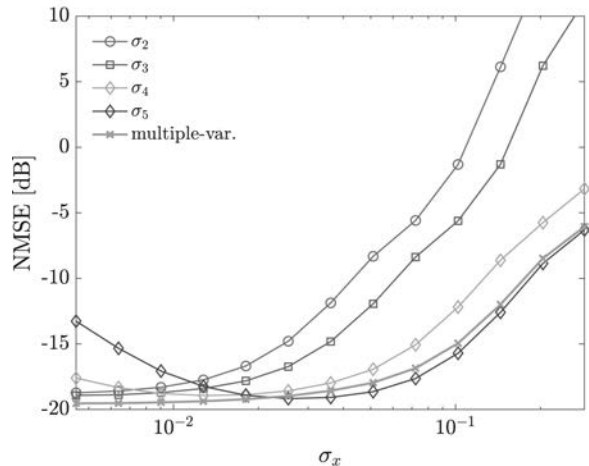
$$M_1 = 64, M_2 = 32, M_3 = 32, \quad (21)$$

where M_j is the memory of the Wiener and Volterra kernels of order j .

Fig. 2 shows the first order kernel of the multiple-variance Volterra model in time (Fig. 2(a)) and frequency



(a)



(b)

Fig. 3. NMSE of complete Volterra models of Roma 27AC. (a) WGN input, (b) music input.

domain (Fig. 2(b)) respectively. The range of time values in the x-axis of Fig. 2(a) corresponds to the memory value, $M_1 = 64$, multiplied for the sampling time $\tau_{\max} = 64/44100 = 1.45$ ms. Fig. 2(b) also shows the power spectrum of the first order kernel of the single-variance Volterra model, identified with the maximum variance, σ_5^2 .

Fig. 3 shows the NMSE of the single-variance Volterra models and that of the multiple-variance Volterra model, as a function of input standard deviation. The Figure was obtained by using as testing input of the Volterra models each of the white noise signals belonging to the testing set shown in Fig. 1(b), and calculating the NMSE for each of them. In the Figure you can count 13 NMSE points for each curve, one for each of the white noise input signals.

In Fig. 3(a) we can see that the error curve related to the multiple-variance method interpolates the inferior values of the curves for single-variances, as the multiple-variance method was meant to do.

The single-variance Volterra models have performance similar to the multiple-variance one only in a short interval around the variance used for the measurement, while

Table 3. Parameters of reduced Volterra models of Roma 27AC.

| memory | delay |
|------------|------------|
| $M_1 = 64$ | $D_1 = 0$ |
| $M_2 = 15$ | $D_2 = 19$ |
| $M_3 = 11$ | $D_3 = 21$ |

outside this interval the error increases up to 15 dB. It should be noticed that the proposed model has a NMSE always less than -25 dB.

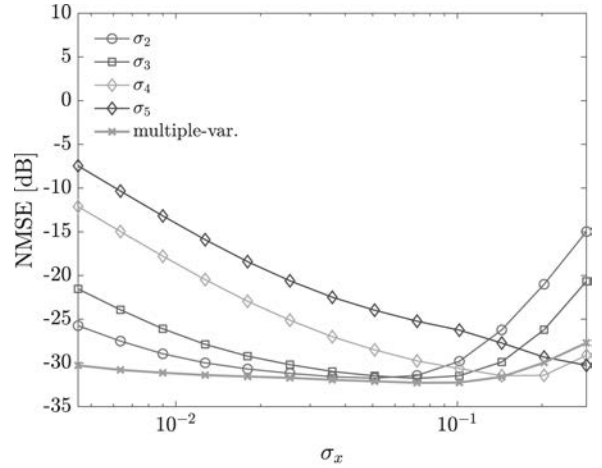
Fig. 3(b) shows similar curves but obtained with the music inputs reported in Fig. 1(b). Also in this Figure the multiple-variance curve approaches the inferior values of the curves for single-variances, although the single-variance model identified with σ_5 goes better for some inputs, reaching the best performance difference of -0.79 dB, but for low variances it performs worse until 6.3 dB.

Each of the Volterra models with the kernel memories reported in Eq. (21) has a total of 6577 kernel elements. This can make their real-time implementation very difficult. With the aim of reducing the complexity of Volterra models we have applied the procedure described at the end of the Sec. 2, that consists in reducing the memory extent of the kernel, keeping a reduced number of kernel values around the peak of the same kernel. The reduced Volterra models, that we have found to have comparable performance to the complete model, have the parameters reported in Table 3, where the D_j are kernel delays, as defined in Eq. (14). The reduced models have now just 454 kernel elements and can thus be easily implemented in real-time.

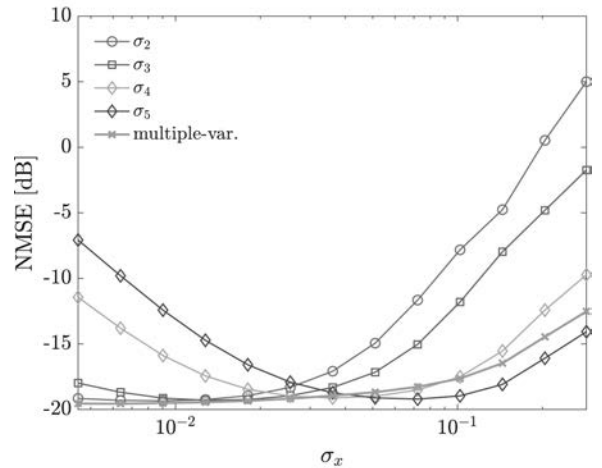
Fig. 4(a) shows the performance of the reduced-memory Volterra models obtained using white noise inputs. In comparison with Fig. 3(a), we can see an improvement of single-variance model performance for high input variances and a worsening for small input variances. This can be explained by considering that, in the reduced kernel models, even though all the neglected elements of higher order kernels could contain some missing information about the kernel, in most cases they contain identification noise. This higher order kernel noise becomes relevant for high power inputs (so avoiding it improves the performance), but it is less relevant for low variance inputs, where the missing information prevails. The multiple-variance method, having much less identification error, is much less affected from the kernel truncation, maintaining the same performance at low input variance and performing a little better only for high input variances.

Similar results are also shown in Fig. 4(b) that reports the NMSE obtained with music input. Here, the single-variance model identified with σ_5 , achieved a better performance difference of 1.6 dB, with respect the multiple-variance one, but a worse performance difference of 12.5 dB.

Fig. 5 shows the values of the second-order Volterra kernel of the multiple-variance method that have been estimated in the reduced model. It can be noticed that the kernel elements shown in the Figure start from 4.3 ms, corresponding to $D_2 = 19$ samples.



(a)



(b)

Fig. 4. NMSE of reduced Volterra models of Roma 27AC. (a) WGN input, (b) music input.

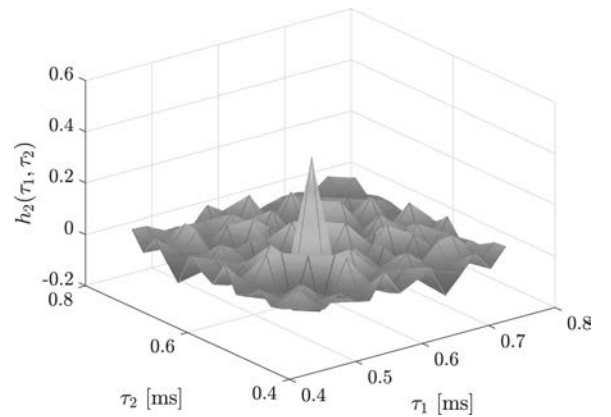
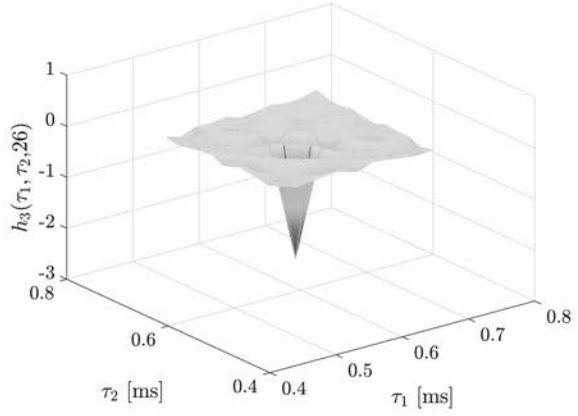
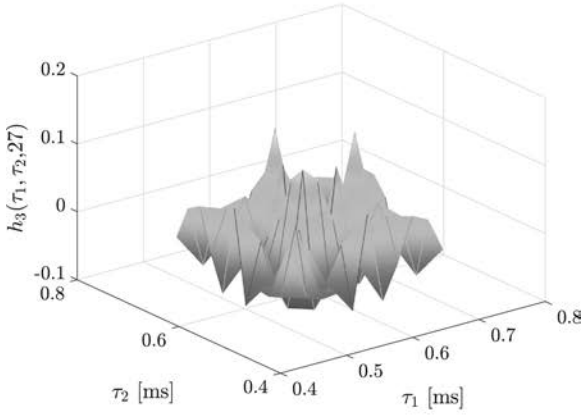


Fig. 5. Roma 27AC: second order Volterra kernel, $h_2(\tau_1, \tau_2)$.

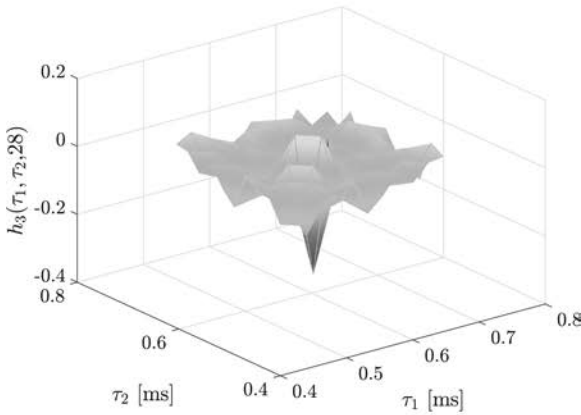
Fig. 6 shows three slices of the third order kernel of the multiple-variance Volterra model. The third order kernel of the reduced model has a delay similar to the second order one ($D_3 = 21$ samples) but a smaller memory, $M_3 = 11$.



(a)



(b)



(c)

Fig. 6. Roma 27AC: third order Volterra kernel $h_3(\tau_1, \tau_2, \tau_3)$.

3.3 SI Audio OTL509/25 Identification Results

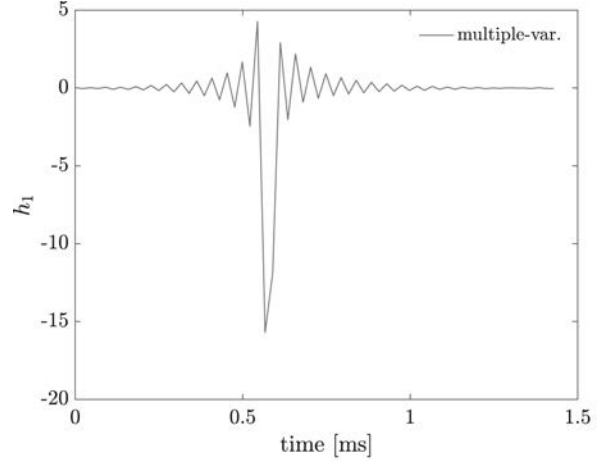
In the second experiment the SI audio vacuum-tube amplifier was identified. Also in this case, four single-variance and one multiple-variance Volterra models were identified. The models were of the fourth order. In the multiple-variance method each kernel was identified with the input variances reported in Table 4.

The memory of the kernels of all the identified Volterra models were

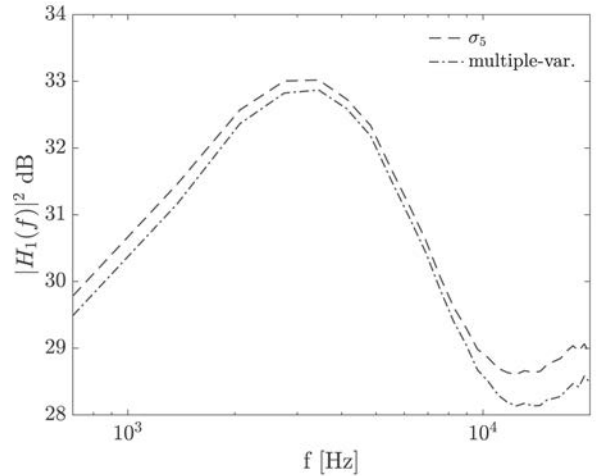
$$M_1 = 64, M_2 = 34, M_3 = 32, M_4 = 29. \quad (22)$$

Table 4. Variances used in the multiple-variance estimation method.

| kernel | input variance |
|--------|----------------|
| k_0 | σ_1^2 |
| k_1 | σ_2^2 |
| k_2 | σ_3^2 |
| k_3 | σ_4^2 |
| k_4 | σ_5^2 |



(a)

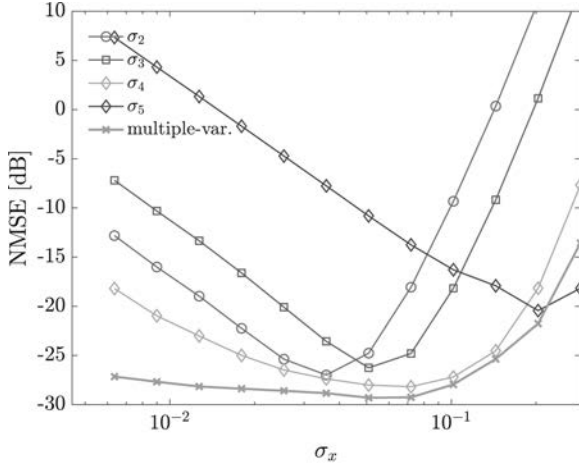


(b)

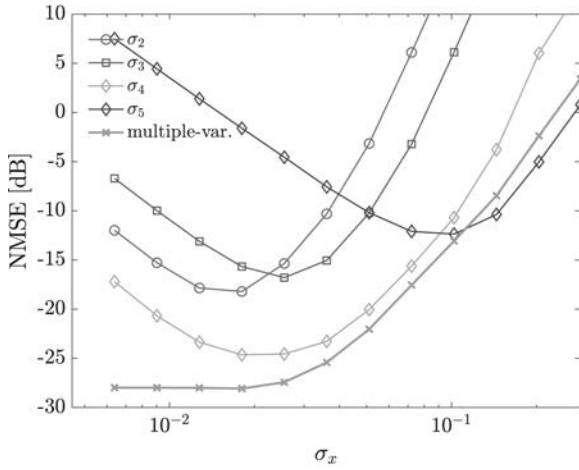
Fig. 7. OTL509/25: first order Volterra kernel (a) in time domain ($h_1(\tau)$) (b) in frequency domain ($|H_1(f)|^2$).

Figs. 7(a) and 7(b) show the Volterra model of the first order, in time and frequency domain, respectively. Fig. 7(b) also shows the power spectrum of the first order model obtained by the single-variance Volterra model, identified at the maximum variance, σ_5^2 . It can be noticed a flat response, a magnitude of $H_1(f)$ of about 30 dB that, considering the attenuation of the D/A converter, corresponds to a gain of 36 dB.

Fig. 8 shows the NMSE of the single-variance Volterra models and of the multiple-variance Volterra model, as a function of input standard deviation. The Figure was



(a)



(b)

Fig. 8. NMSE of complete Volterra models of OTL509/25. (a) WGN input, (b) music input.

obtained by using as input of the Volterra models each of the white noise signals belonging to the testing set, shown in Fig. 1(b), and calculating the NMSE for each of them.

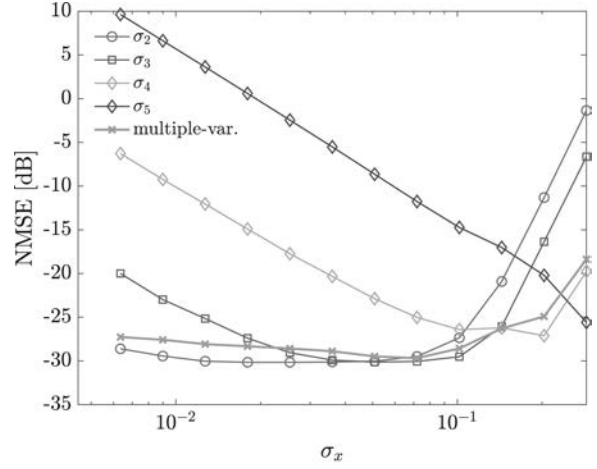
Fig. 8(a) shows that, also in this experiment, the error curve of the multiple-variance Volterra models interpolates the inferior values of the errors of the single-variance models, apart for the single-variance models with σ_5 , which goes better at the point of maximum variance but performs worse up to 30 dB at low variances.

Fig. 8(b) shows similar curves, but obtained with the music inputs of Fig. 1(b). Also in this Figure the multiple-variance method interpolates the inferior values of the single-variance one, although the single-variance model identified with σ_5 , goes better for some inputs, with the best performance difference of -2.6 dB, but for low variances it performs worse until 35.5 dB of difference.

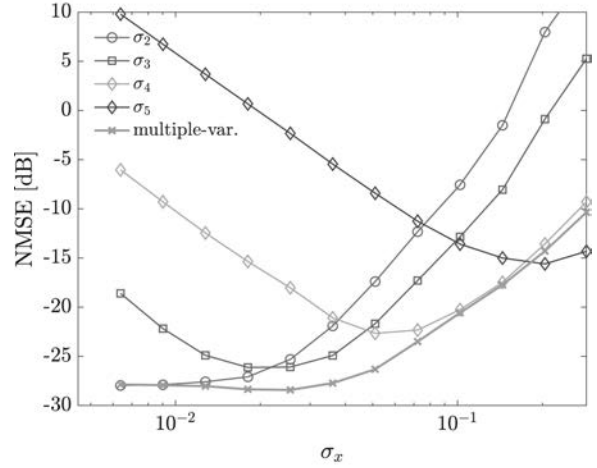
Each of these Volterra models, with the kernel memories reported in Eq. (22), has a total of 42604 kernel elements. Consequently, also in this experiment we have applied the procedure described at the end of the Sec. 2 to reduce the number of kernel elements. The reduced Volterra models

Table 5. Parameters of reduced Volterra models of OTL509/25.

| memory | delay |
|------------|------------|
| $M_1 = 64$ | $D_1 = 0$ |
| $M_2 = 15$ | $D_2 = 19$ |
| $M_3 = 11$ | $D_3 = 21$ |
| $M_4 = 5$ | $D_4 = 24$ |



(a)



(b)

Fig. 9. NMSE of reduced Volterra models of OTL509/25. (a) WGN input, (b) music input.

that we have found have performance comparable to the complete models have parameters reported in Table 5.

The reduced models have now just 541 kernel elements and can be easily implemented in real-time.

Figs. 9(a) and 9(b) show the performance of the reduced-memory Volterra models, obtained using white noise and music inputs, respectively. Also in this experiment, in comparison with Fig. 8 we can see a performance improvement of the single-variance Volterra model σ_5 for high input variances and a worsening for small input variances. In Fig. 9(a) we can see that in some small variance intervals the single-variance Volterra models perform slightly

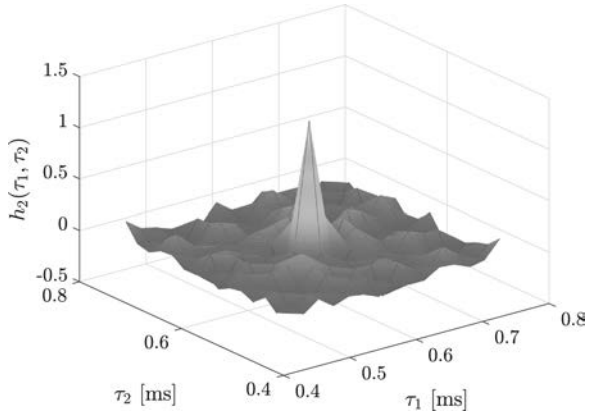


Fig. 10. OTL509/25: second order Volterra kernel ($h_2(\tau_1, \tau_2)$).

Table 6. Variances used in the multiple-variance estimation method.

| kernel | input variance |
|--------|----------------|
| k_0 | σ_1^2 |
| k_1 | σ_2^2 |
| k_2 | σ_4^2 |
| k_3 | σ_5^2 |

better than the multiple-variance one but perform definitely worse for other variance values. In Fig. 9(b) the multiple-variance Volterra model approaches better the inferior values of single-variance models.

Fig. 10 shows the second-order kernel that is used in the reduced multiple-variance Volterra model. The elements shown in Figure start from 4.3 ms ($D_2 = 19$).

Fig. 11 shows three slices of the third order kernel of the reduced multiple-variance Volterra model. The third order kernel has a delay similar to the second order one but a smaller memory, $M_3 = 11$.

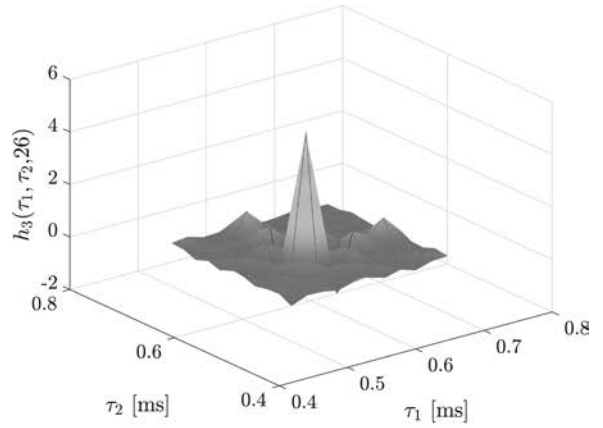
3.4 Presonus TubePre Identification Results

In the last experiment the Presonus TubePre microphone pre-amplifier was identified. Four single-variance Volterra models and a multiple-variance model of the third order were first identified. Each kernel of the multiple-variance model was identified with a different variance as shown in Table 6.

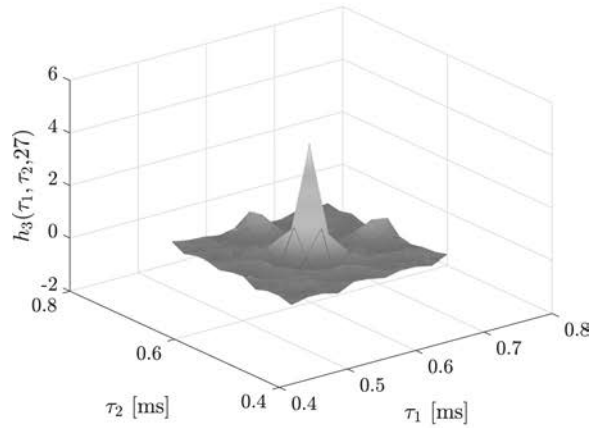
The memory of the kernels of all the Wiener and Volterra models are

$$M_1 = 50, M_2 = 35, M_3 = 35. \quad (23)$$

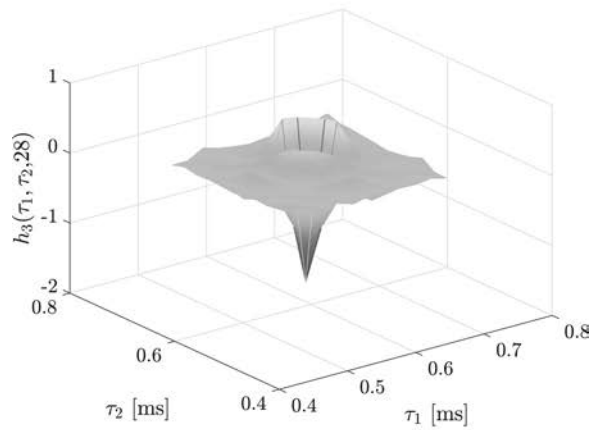
Figs. 12(a) and 12(b) show the Volterra model of the first order, in time and frequency domain, respectively. Fig. 12(b) also shows the power spectrum of the first order model obtained by the single-variance Volterra model, identified at the maximum variance, σ_5^2 . It can be noticed that, while Figs. 2(b) and 7(b) correspond to amplifier gains of about 36 dB, the magnitude of TubePre, considering the attenuation of the A/D converter, corresponds to a 20 dB gain.



(a)



(b)

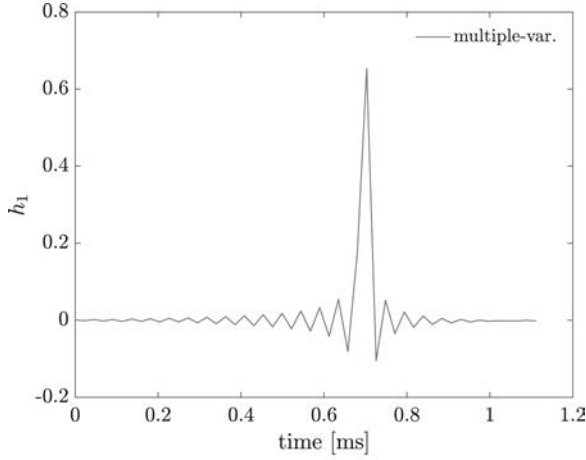


(c)

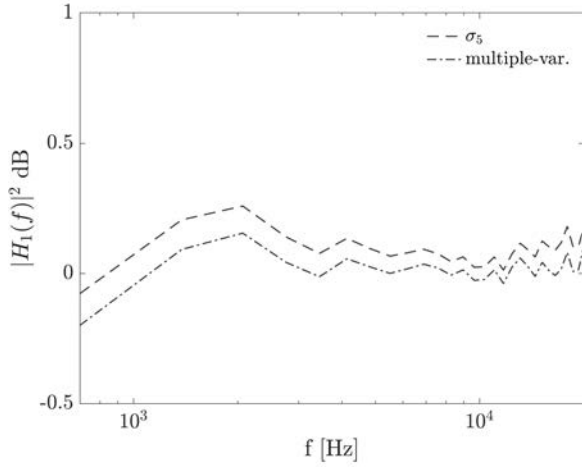
Fig. 11. OTL509/25: third order Volterra kernel ($h_3(\tau_1, \tau_2, \tau_3)$).

Fig. 13 shows the NMSE of single-variance Volterra models and that of the multiple-variance Volterra model, as a function of input standard deviation. Fig. 13 shows the best performance of the multiple-variance methodology in the three amplifier identifications, in fact the NMSE of the multiple-variance Volterra model is always smaller than that of the single-variance Volterra models.

Each of these Volterra models, with the kernel memories reported in Eq. (23), has a total of 8451 kernel elements. Also in this case we have applied the procedure described



(a)



(b)

Fig. 12. TubePre: first order Volterra kernel (a) in time domain ($h_1(\tau)$) (b) in frequency domain ($|H_1(f)|^2$).

Table 7. Parameters of reduced Volterra models of TubePre.

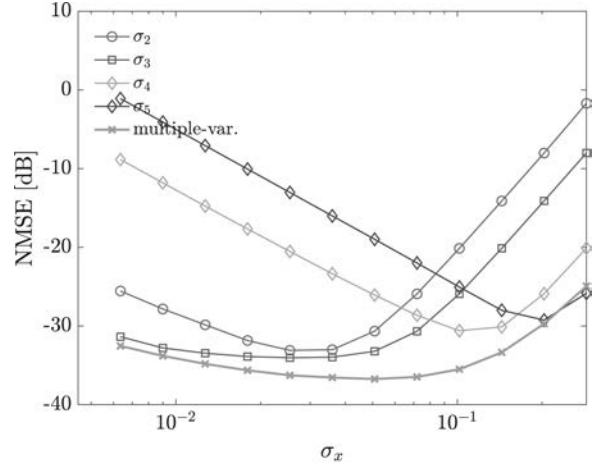
| memory | delay |
|------------|------------|
| $M_1 = 50$ | $D_1 = 0$ |
| $M_2 = 9$ | $D_2 = 26$ |
| $M_3 = 9$ | $D_3 = 26$ |

at the end of the Sec. 2, to reduce the number of kernel elements. The reduced Volterra models, that we have found to have performance comparable to the complete ones, have the parameters in Table 7. In this case the reduced models have just 261 kernel elements.

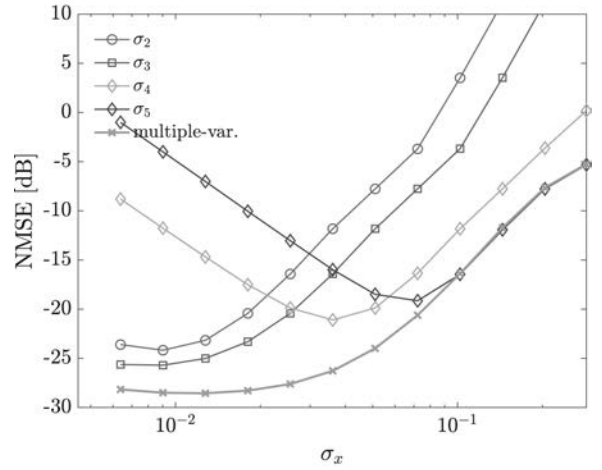
Figs. 14(a) and 14(b) show the performance of the reduced-memory Volterra models, obtained using white noise and music inputs, respectively. The best performance shown in Fig. 13 is maintained also for the reduced multiple-variance Volterra models.

Fig. 15 shows the values of second-order kernel identified in the reduced multiple-variance Volterra model. The elements shown in the Figure start from 4.3 ms ($D_2 = 19$).

Fig. 16 shows three slices of the third order kernel of the



(a)



(b)

Fig. 13. NMSE of complete Volterra models of TubePre for (a) WGN input, (b) music input.

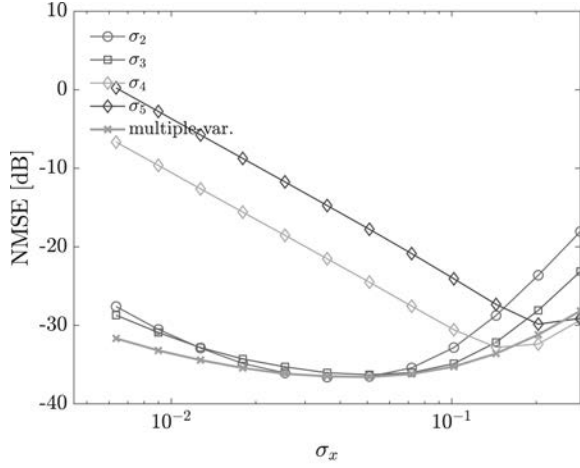
Table 8. Comparison between the number of kernel elements required by the complete Volterra model and by the reduced one, for the identified amplifiers.

| Amplifier | Model order | Number of kernel elements | |
|-----------|-------------|---------------------------|---------------|
| | | Complete model | Reduced model |
| Synthesis | 3 | 6577 | 471 |
| SI Audio | 4 | 42604 | 541 |
| Presonus | 3 | 8451 | 261 |

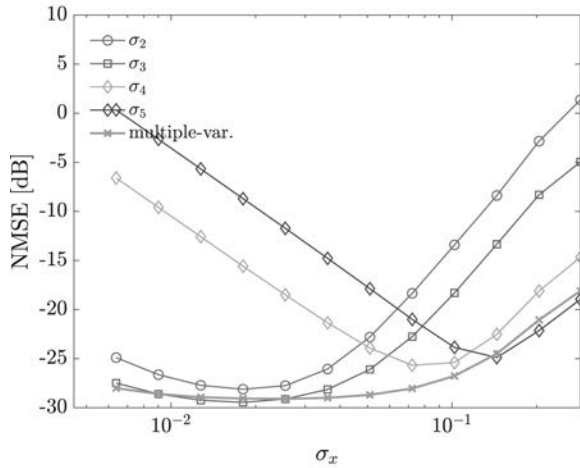
reduced multiple-variance Volterra model. The third order kernel has a delay and memory equal to the second order one.

3.5 Discussion

Table 8 shows the number of kernel elements of the complete models and of the reduced ones for all the three experiments. A reduction in the number of elements of one order of magnitude for the third order models and of two



(a)



(b)

Fig. 14. NMSE of complete Volterra models of TubePre for (a) WGN input, (b) music input.

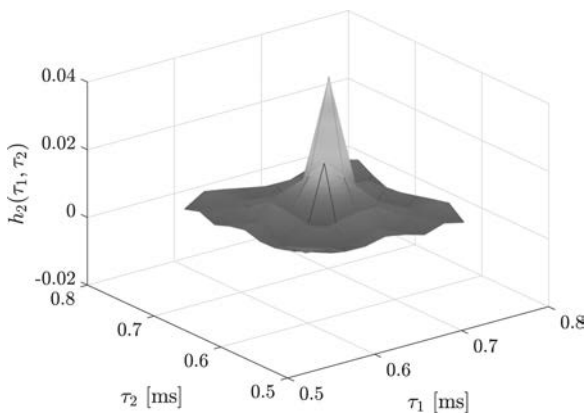
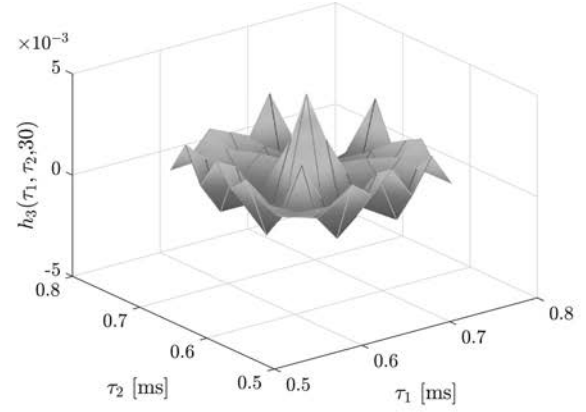


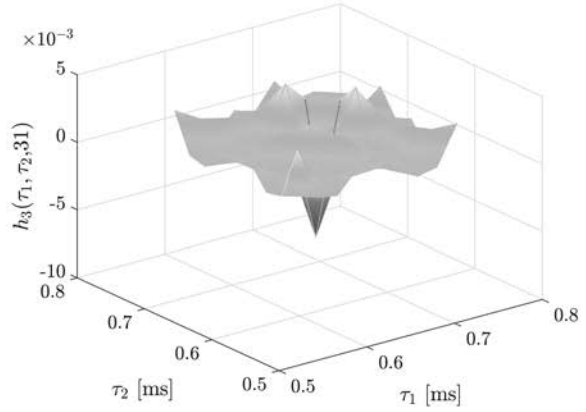
Fig. 15. TubePre: second order Volterra kernel, $h_2(\tau_1, \tau_2)$.

order of magnitude for the fourth order one can be achieved. As it can be seen by comparing Figs. 3 and 4, Figs. 8 and 9, and finally Figs. 13 and 14, if the multiple-variance methodology is used this reduction in complexity can be realized without worsening the identification performance.

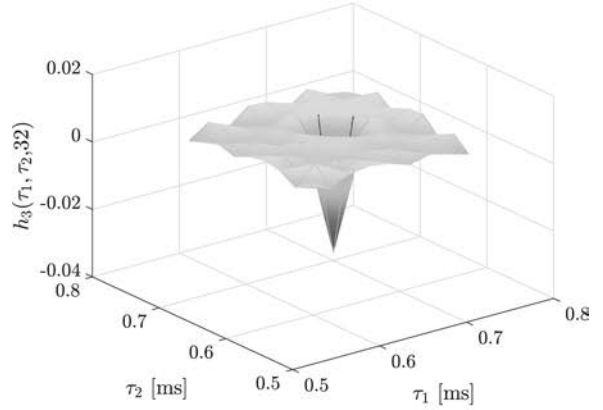
This complexity reduction makes it possible to do a real time implementation of the proposed models. Using a filter



(a)



(b)



(c)

Fig. 16. TubePre: third order Volterra kernel $h_3(\tau_1, \tau_2, \tau_3)$.

bank implementation for the Volterra filter [41], a kernel of order P and memory M requires $\binom{M+P-2}{P-1}$ multiplications for computing the input samples cross-products and $\binom{M+P-1}{P-1}$ multiply-accumulate (MAC) operations for the filter bank operations. Many attempts have been made to reduce this number, by a proper combination of the operations, either in time [42, 43] or in frequency domain [44–46]. Regardless of these techniques, Table 9 reports the number of MAC required by each proposed model per each sample and the million of MAC per second (MMACS), by using a filter bank implementation. Each multiplication

Table 9. Number of operations required for a filter bank implementation of Volterra filters.

| Amplifier | Model order | Complete model | | Reduced Model | |
|-----------|-------------|----------------|--------|----------------|-------|
| | | MAC per sample | MMACS | MAC per sample | MMACS |
| Synthesis | 3 | 7664 | 338.0 | 617 | 27.2 |
| SI Audio | 4 | 57178 | 2521.5 | 792 | 34.9 |
| Presonus | 3 | 9745 | 429.8 | 359 | 15.8 |

used for computing the input samples cross-products is counted as a MAC. It can be noticed that the reduced models, which provides the same modeling performance of the complete ones, are affordable by most of the DSPs on the market. On the contrary, the complete models provide an unacceptable computational burden.

4 CONCLUSION

In this paper it was shown through extensive experiments that the multiple-variance identification method can be effectively used to derive Volterra models of different audio devices. The multiple-variance method allows to avoid the problem of locality of the solution as shown in the Figures reporting the NMSE of single-variance and multiple-variance Volterra models. Indeed, the Figures clearly show how the NMSE of multiple-variance Volterra models interpolates the inferior NMSE values of the single-variance models. As a matter of fact, the obtained models can emulate audio devices on a wide range of input signal powers.

A technique to reduce the number of elements of Wiener and Volterra kernels has also been proposed to contrast the curse of dimensionality and a procedure for their identification has been presented. The reduced models identified with the multiple variance method provide an effective mean to emulate nonlinear audio devices in real-time applications.

5 ACKNOWLEDGMENT

This work was partially supported by a DII Research Grant and a DiSPeA Research Grant.

6 REFERENCES

[1] V. Volterra, *Theory of Functionals and of Integrals and Integro-Differential Equations* (Dover Publications, New York, 1959).

[2] N. Wiener, *Nonlinear Problems in Random Theory* (John Wiley, New York, 1958).

[3] M. B. Brilliant, "Theory of the Analysis of Nonlinear Systems," RLE Technical Report 345, MIT, Cambridge, MA (1958).

[4] Y. W. Lee and M. Schetzen, "Measurement of the Wiener Kernels of a Nonlinear System by Crosscorrelation," *Int. J. Control*, vol. 2, no. 3, pp. 237–254 (1965 Sep.).

[5] W. Rudin, *Principles of Mathematical Analysis* (McGraw-Hill, New York, 1976).

[6] M. Pirani, S. Orcioni, and C. Turchetti, "Diagonal Kernel Point Estimation of n-th Order Discrete Volterra-Wiener Systems," *EURASIP J. Applied Signal Processing*, vol. 2004, no. 12, pp. 1807–1816 (2004 Sep.).

[7] S. Orcioni, M. Pirani, and C. Turchetti, "Advances in Lee-Schetzen Method for Volterra Filter Identification," *Multidimensional Systems and Signal Processing*, vol. 16, no. 3, pp. 265–284 (2005).

[8] S. Orcioni, "Improving the Approximation Ability of Volterra Series Identified with a Cross-Correlation Method," *Nonlinear Dynamics*, vol. 78, no. 4, pp. 2861–2869 (2014 Sep.), doi: <https://doi.org/10.1007/s11045-004-1677-7>.

[9] A. Carini, L. Romoli, S. Cecchi, and S. Orcioni, "Perfect Periodic Sequences for Nonlinear Wiener Filters," *2016 24th European Signal Processing Conference (EUSIPCO)*, pp. 1788–1792 (2016 Aug.), doi: <https://doi.org/10.1109/EUSIPCO.2016.7760556>.

[10] S. Orcioni, S. Cecchi, and A. Carini, "Multi-variance Nonlinear System Identification Using Wiener Basis Functions and Perfect Sequences," *2017 25th European Signal Processing Conference (EUSIPCO)*, pp. 2748–2752 (2017 Aug), doi: <https://doi.org/10.23919/EUSIPCO.2017.8081697>.

[11] V. J. Mathews and G. L. Sicuranza, *Polynomial Signal Processing* (Wiley, New York, 2000).

[12] J. Pakarinen and D. T. Yeh, "A Review of Digital Techniques for Modeling Vacuum-Tube Guitar Amplifiers," *Computer Music J.*, vol. 33, no. 2, pp. 85–100 (2009), doi: <https://doi.org/10.1162/comj.2009.33.2.85>.

[13] T. I. Karimov, D. N. Butusov, and A. I. Karimov, "Computer Simulation of Audio Circuits with Vacuum Tubes," *2016 XIX IEEE International Conference on Soft Computing and Measurements (SCM)*, pp. 114–116 (2016 May), doi: <https://doi.org/10.1109/SCM.2016.7519700>.

[14] M. Karjalainen and J. Pakarinen, "Wave Digital Simulation of a Vacuum-Tube Amplifier," *2006 IEEE International Conference on Acoustics Speech and Signal Processing Proceedings*, vol. 5, pp. V–V (2006 May), doi: <https://doi.org/10.1109/ICASSP.2006.1661235>.

[15] W. R. Dunkel, M. Rest, K. J. Werner, M. J. Olsen, and J. O. Smith, "The Fender Bassman 5F6-A family of Preampifier Circuits—A Wave Digital Filter Case Study," *Proceedings of the 19th International Conference on Digital Audio Effects*, p. 263–270 (2016).

[16] T. Schmitz and J.-J. Embrechts, "Hammerstein Kernels Identification by Means of a Sine Sweep

Technique Applied to Nonlinear Audio Devices Emulation,” *J. Audio Eng. Soc.*, vol. 65, pp. 696–710 (2017 Sep.), <http://www.aes.org/e-lib/browse.cfm?elib=19200>.

[17] M. Scarpiniti, D. Comminiello, R. Parisi, and A. Uncini, “Comparison of Hammerstein and Wiener Systems for Nonlinear Acoustic Echo Cancelers in Reverberant Environments,” *2011 17th International Conference on Digital Signal Processing (DSP)*, pp. 1–6 (2011 July), doi:<https://doi.org/10.1109/ICDSP.2011.6004959>.

[18] F. Eichas, S. Möller, and U. Zölzer, “Block-Oriented Gray Box Modeling of Guitar Amplifiers,” *Proceedings of the 20th International Conference on Digital Audio Effects (DAFx-17)*, pp. 184–191 (2017 Sep. 5–9).

[19] F. Eichas, E. Gerat, and U. Zölzer, “Virtual Analog Modeling of Dynamic Range Compression Systems,” presented at the *142nd Convention of the Audio Engineering Society* (2017 May), convention paper 9752, <http://www.aes.org/e-lib/browse.cfm?elib=18628>.

[20] E. Gerat, F. Eichas, and U. Zölzer, “Virtual Analog Modeling of a UREI 1176LN Dynamic Range Control System,” presented at the *143rd Convention of the Audio Engineering Society* (2017 Oct.), convention paper 9852, <http://www.aes.org/e-lib/browse.cfm?elib=19249>.

[21] C. Hofmann, C. Huemmer, and W. Kellermann, “Significance-Aware Hammerstein Group Models for Nonlinear Acoustic Echo Cancellation,” *2014 IEEE International Conference on Acoustics, Speech and Signal Processing (ICASSP)*, pp. 5934–5938 (2014 May), doi:<https://doi.org/10.1109/ICASSP.2014.6854742>.

[22] C. Huemmer, C. Hofmann, R. Maas, and W. Kellermann, “The Significance-Aware EPFES to Estimate a Memoryless Preprocessor for Nonlinear Acoustic Echo Cancellation,” *2014 IEEE Global Conference on Signal and Information Processing (GlobalSIP)*, pp. 557–561 (2014 Dec.), doi:<https://doi.org/10.1109/GlobalSIP.2014.7032179>.

[23] C. Hofmann, M. Guenther, C. Huemmer, and W. Kellermann, “Efficient Nonlinear Acoustic Echo Cancellation by Partitioned-Block Significance-Aware Hammerstein Group Models,” *2016 24th European Signal Processing Conference (EUSIPCO)*, pp. 1783–1787 (2016 Aug.), doi:<https://doi.org/10.1109/EUSIPCO.2016.7760555>.

[24] C. Hofmann, C. Huemmer, M. Guenther, and W. Kellermann, “Significance-Aware Filtering for Nonlinear Acoustic Echo Cancellation,” *EURASIP J. Advances in Signal Processing*, vol. 2016, no. 1, p. 113 (2016 Nov.), doi: <https://doi.org/10.1186/s13634-016-0410-7>.

[25] A. Novák, “Identification of Nonlinear Systems: Volterra Series Simplification,” *Acta Polytechnica*, vol. 47, no. 4, pp. 72–75 (2007 May).

[26] F. T. Agerkvist, “Volterra Series Based Distortion Effect,” presented at the *129th Convention of the Audio Engineering Society* (2010 Nov.), convention paper 8212, <http://www.aes.org/e-lib/browse.cfm?elib=15634>.

[27] F. Eichas, S. Möller, and U. Zölzer, “Block-Oriented Modeling of Distortion Audio Effects Using Iterative Minimization,” *Proceedings of the 20th International Conference on Digital Audio Effects (DAFx-15)* (2015 Nov. 30–Dec. 3).

[28] M. Holters, K. Dempwolf, and U. Zölzer, “A Digital Emulation of the Boss SD-1 Super Overdrive Pedal Based on Physical Modeling,” presented at the *131st Convention of the Audio Engineering Society* (2011 Oct.), convention paper 8506, <http://www.aes.org/e-lib/browse.cfm?elib=16032>.

[29] D. T. Yeh, J. Abel, and J. O. Smith, “Simulation of the Diode Limiter in Guitar Distortion Circuits by Numerical Solution of Ordinary Differential Equations,” *Proc. of the 10th Int. Conference on Digital Audio Effects (DAFx-07)* (2007 Sep. 10–15).

[30] T. Schmitz and J. J. Embrechts, “Nonlinear Guitar Loudspeaker Simulation,” presented at the *134th Convention of the Audio Engineering Society* (2013 May), e-Brief 96, <http://www.aes.org/e-lib/browse.cfm?elib=16697>.

[31] T. Hélie, “On the Use of Volterra Series for Real-Time Simulations of Weakly Nonlinear Analog Audio Devices: Application to the Moog Ladder Filter,” *Proceedings of the 9th International Conference on Digital Audio Effects (DAFx06)*, pp. 7–12 (2006).

[32] D. Bard, “Horn Loudspeakers Nonlinearity Comparison and Linearization Using Volterra Series,” presented at the *124th Convention of the Audio Engineering Society* (2008 May), convention paper 7318, <http://www.aes.org/e-lib/browse.cfm?elib=14448>.

[33] T. Katayama and M. Serikawa, “Reduction of Second Order Non-Linear Distortion of a Horn Loudspeaker by a Volterra Filter-Real-Time Implementation,” presented at the *103rd Convention of the Audio Engineering Society* (1997 Sep.), convention paper 4525.

[34] I. J. Leontaritis and S. A. Billings, “Input-Output Parametric Models for Non-Linear Systems Part I: Deterministic Non-Linear Systems,” *Intl. J. Control*, vol. 41, no. 2, pp. 303–328 (1985), doi: <https://doi.org/10.1080/0020718508961129>.

[35] A. Dobrucki and P. Pruchnicki, “Application of the NARMAX-Method for Modeling of the Nonlinearity of Dynamic Loudspeakers,” presented at the *106th Convention of the Audio Engineering Society* (1999 May), convention paper 4868.

[36] A. Dobrucki and P. Pruchnicki, “Application of the NARMAX Method to the Modeling of the Nonlinearity of Dynamic Loudspeakers,” *Archives of Acoustics*, vol. 26, no. 4 (2001 Jan.). Available at: <http://acoustics.ippt.gov.pl/index.php/aa/article/view/406>.

[37] J. Schattschneider and U. Zölzer, “Discrete-Time Models for Nonlinear Audio Systems,” presented at the *Proceedings of the 2nd COST G-6 Workshop on Digital Audio Effects (DAFx99)* (1999 Dec.).

[38] L. Tronchin, V. L. Coli, and F. F. Gionfalo, “Modeling Nonlinearities on Musical Instruments by Means of Volterra Series,” presented at the *142nd Convention of the Audio Engineering Society* (2017 May), convention paper 9781, <http://www.aes.org/e-lib/browse.cfm?elib=18657>.

[39] L. Tronchin, “Non Linear Convolution and its Application to Audio Effects,” presented at the *131st Convention of the Audio Engineering Society* (2011 Oct.), convention paper 8524, <http://www.aes.org/e-lib/browse.cfm?elib=16050>.

- [40] H. Olesen, "Properties and Units in the Clinical Laboratory Sciences. I. Syntax and Semantic Rules IUPAC-IFCC Recommendations 1995," *Clinica Chimica Acta*, vol. 245, no. 2, pp. S5–S21 (1996), doi: [https://doi.org/10.1016/0009-8981\(96\)85128-X](https://doi.org/10.1016/0009-8981(96)85128-X).
- [41] G. L. Sicuranza and A. Carini, "On a Class of Nonlinear Filters," in M. G. I. Tabus, K. Egiazarian (Ed.), *Festschrift in Honor of Jaakko Astola on the Occasion of his 60th Birthday*, vol. TICSP Report #47, pp. 115–144 (2009).
- [42] H. Enzinger, K. Freiberger, G. Kubin, and C. Vogel, "Fast Time-Domain Volterra Filtering," *2016 50th Asilomar Conference on Signals, Systems and Computers*, pp. 225–228 (2016 Nov.), doi: <https://doi.org/10.1109/ACSSC.2016.7869029>.
- [43] M. M. Banat, "Pipelined Volterra Filter," *Electronics Letters*, vol. 28, no. 13, pp. 1276–1278 (1992 June), doi: <https://doi.org/10.1049/el:19920808>.
- [44] M. J. Reed and M. O. Hawksford, "Efficient Implementation of the Volterra Filter," *IEE Proceedings - Vision, Image and Signal Processing*, vol. 147, no. 2, pp. 109–114 (2000 Apr.), doi: <https://doi.org/10.1049/ip-vis:20000183>.
- [45] M. Morhac, "A Fast Algorithm of Nonlinear Volterra Filtering," *IEEE Transactions on Signal Processing*, vol. 39, no. 10, pp. 2353–2356 (1991 Oct.), doi: <https://doi.org/10.1109/78.91194>.
- [46] R. Bernardini, "A Fast Algorithm for General Volterra Filtering," *IEEE Transactions on Communications*, vol. 48, no. 11, pp. 1853–1864 (2000 Nov.), doi: <https://doi.org/10.1109/26.886476>.

THE AUTHORS



Simone Orcioni



Alessandro Terenzi



Stefania Cecchi



Francesco Piazza



Alberto Carini

Simone Orcioni received his Laurea degree and Ph.D. in electronics engineering from the Università Politecnica delle Marche, where he was a Research Assistant. Since 2000 he has been an Assistant Professor teaching courses in analogue and digital electronics and publishing a textbook. In 2017 he was guest professor at HTWG, Hochschule Konstanz. He has published more than a hundred international papers in journals and conference proceedings and edited four international books. He has been working in statistical device modeling and simulation, analog circuit design, system level simulation, and linear and nonlinear system identification. His current research interests include digital signal processing, in particular nonlinear filtering. Dr. Orcioni is a Senior Member of the Institute of Electrical and Electronics Engineers (IEEE) and a Member of EURASIP.

Alessandro Terenzi was born in Senigallia, Italy, in 1991. He received the Laurea degree (with honors) in electronic engineering in July 2016 at the Polytechnic University of Marche (Italy). He is now a Ph.D student at DII (Department of Information Engineering) at the same university since November 2017. His current research interests are in the area of digital signal processing, including nonlinear audio system and audio processing.

Stefania Cecchi was born in Amandola, Italy, in 1979. She received the Laurea degree (with honors) in electronic engineering from the University of Ancona (now Università Politecnica delle Marche, Italy) in 2004 and the Ph.D. degree in electronic engineering from the University Politecnica delle Marche (Ancona, Italy) in 2007. She was a Post Doc Researcher at DII (Department of Information Engineering) at the same university from February 2008 to October 2015. She is an Assistant Professor at the same department since November 2015. She is the author or coauthor of several international papers. Her current research interests are in the area of digital signal processing, including adaptive DSP algorithms and circuits, speech, and audio processing. Dr. Cecchi is a member of the Audio Engineering Society (AES), Institute of Electrical and Electronics Engineers (IEEE), Italian Acoustical Association (AIA).

Francesco Piazza was born in Italy in 1957. He received the Laurea degree (with honors) in electronic engineering from the University of Ancona (now Università Politecnica delle Marche, Italy) in 1981. From 1981 to 1983 he worked on image processing in the Physics Department at the University of Ancona. After a stint at the Olivetti OSAI Software Development Center, Ivrea, Italy, he joined the Department of Electronics and Automatics, University of Ancona, in 1985, first as a researcher in electrical engineering, then as an associate professor. Currently, he is a full professor at the Università Politecnica delle Marche (Ancona, Italy). He is the author and coauthor of more than 200 international papers. His current research interests are in the areas of circuit theory and digital signal processing, including adaptive DSP algorithms and circuits, artificial neural networks, speech, and audio processing. Prof. Piazza is a member of IEEE and an associate member of the Audio Engineering Society.

Alberto Carini received the Laurea degree (summa cum laude) in electronic engineering and the Dottorato di Ricerca (Ph.D.) degree in information engineering from the University of Trieste in 1994 and 1998, respectively. In 1996 and 1997, during his doctoral studies, he was a Visiting Scholar with the University of Utah, Salt Lake City. From 1997 to 2003, he was a DSP Engineer with Telit Mobile Terminals SpA, Trieste, where he led audio processing R&D activities. In 2003 he was with Neonseven srl, Trieste, as an audio and DSP expert. From 2001 to 2004, he collaborated with the University of Trieste as a Contract Professor of digital signal processing. Since 2004, he has been an Associate Professor with the University of Urbino, Urbino, Italy. His research interests include system identification, adaptive filtering, nonlinear filtering, nonlinear equalization, acoustic echo cancellation, active noise control, room response equalization, and signal processing for road surface monitoring. Dr. Carini is a Senior Member of the IEEE and a Member of EURASIP. Currently, he is an Editorial Board Member of Elsevier Signal Processing, and a Member of SPS Signal Processing Theory and Methods Technical Committee.